Supramolecular Organization of Oligo(*m*-phenylene ethynylene)s in the Solid-State

Peggy-Jean Prest, Ryan B. Prince, and Jeffrey S. Moore*

Contribution from the Departments of Chemistry and Materials Science & Engineering, The University of Illinois at Urbana−Champaign, 600 South Mathews Avenue, Urbana, Illinois 61801

Received March 24, 1999

Abstract: A series of oligo(*m*-phenylene ethylene)s having triethylene glycol ester-linked side chains (i.e., 2-[2-(2-methoxyethoxy)ethoxy]ethyl esters) were prepared, and their supramolecular organization in the solid-state was studied. These oligomers are amphiphilic, having a nonpolar aromatic hydrocarbon backbone that is appended with flexible polar side chains. Oligomers containing eight or more monomers are viscoelastic waxy solids at room temperature, exhibiting birefringent textures that reversibly melt into isotropic fluids upon warming. As the chain length increases, the materials stiffen and the melting point rises asymptotically, suggesting homologous packing for all members of the series. These observations are in accord with the behavior of conventional short-chain polymers, whereby melting point depression results from the volume fraction of chain ends. Small- and wide-angle X-ray diffraction investigations were carried out to elucidate the details of chain packing. Samples slowly cooled from the isotropic melt develop lamellar organizations with longitudinal spacings that depend linearly on the chain length. The relationship between the calculated repeat unit length and the experimentally observed increment in lamellar spacing per repeat unit suggests that the chains are oriented 30° from the layer normal. Macroscopically aligned samples showed two sets of mutually orthogonal lateral reflections whose *d*-spacings are nearly independent of chain length. A model for the solid-state organization of these oligomers is proposed. Solution- and solid-state UV spectra are presented and interpreted by considering the relative abundance of cisoid vs transoid conformers under these various conditions.

Introduction

Phenylene ethynylene architectures have proven to be a rich platform on which to conduct supramolecular and nanoscale chemistry.[1,2] Representative examples as shown in Chart 1 include hexameric macrocycles,[3−7] para-linked rigid rod segments,[8−15] and the more conformationally diverse ortho- and meta-linked oligomers.[16−20] A summary of their observed supramolecular behavior can be gleaned from Figure 1. For example, hexameric macrocycles having appropriate side chains associate in solution to form stacked dimers and higher order aggregates.[21] Recent findings from our laboratory have shown that the strength of the aromatic stacking interactions responsible for these aggregates is strongly dependent on solvent polarity.[22] In the absence of any solvent, these macrocycles behave as extended-core discotic mesogens that self-organize into tubular liquid crystal phases.[23] In many respects, analogous behavior is observed for oligomeric *m*-phenylene ethynylenes. In dilute solutions of "poor" solvents, chains long enough to fold back on themselves adopt helical conformations.[16,18,19] This intramolecular structure is presumably stabilized by π-stacking interactions of a similar nature to those that drive the macrocycles to aggregate in solution. At higher concentrations, long-chain oligomers undergo intermolecular aggregation, as evidenced by severe broadening of NMR signals and by nonideality in vapor pressure osmometry measurements.[16,22] One possible mode of intermolecular association of the helical conformation

* To whom correspondence should be addressed. Phone: (217) 244-4024. Fax: (217) 244-8068. E-mail: moore@scs.uiuc.edu.

(1) Tour, J. M. *Chem. Rev.* **1996**, *96*, 537−553.
(2) Moore, J. S. *Acc. Chem. Res.* **1997**, *30*, 402−413.
(3) Zhang, J.; Pesak, D. J.; Ludwick, J. J.; Moore, J. S. *J. Am. Chem. Soc.* **1994**, *116*, 4227−4239.
(4) Hoger, S.; Spickermann, J.; Morrison, D. L.; Dziezok, P.; Ruder, H. J. *Macromolecules* **1997**, *30*, 3110−3111.
(5) Morrison, D. L.; Hoger, S. *Chem. Commun.* **1996**, *20*, 2313−2314.
(6) Venkataraman, D.; Lee, S.; Zhang, J.; Moore, J. S. *Nature* **1994**, *371*, 591−593.
(7) Shetty, A. S.; Fischer, P. R.; Stork, K. F.; Bohn, P. W.; Moore, J. S. *J. Am. Chem. Soc.* **1996**, *118*, 9409−9411.
(8) Fiesel, R.; Halkyard, C. E.; Rampey, M. E.; Kloppenburg, L.; Studer-Martinez, S. L.; Scherf, U.; Bunz, U. W. F. *Macromol. Rapid Commun.* **1999**, *20*, 107−111.
(9) Wautelet, P.; Moroni, M.; Oswald, L.; Lemoigne, J.; Pham, A.; Bigot, J. Y.; Luzzati, S. *Macromolecules* **1996**, *29*, 446−455.
(10) Ziener, U.; Godt, A. *J. Org. Chem.* **1997**, *62*, 6137−6143.
(11) Samori, P.; Francke, V.; Mangel, T.; Mullen, K.; Rabe, J. P. *Opt. Mater.* **1998**, *9*, 390−393.
(12) Francke, V.; Rader, H. J.; Geerts, Y.; Mullen, K. *Macromol. Rapid. Commun.* **1998**, *19*, 275−281.
(13) Kloppenburg, L.; Song, D.; Bunz, U. H. F. *J. Am. Chem. Soc.* **1998**, *120*, 7973−7974.
(14) Fiesel, R.; Scherf, U. *Macromol. Rapid Commun.* **1998**, *19*, 427−431.
(15) Reinerth, W. A.; Jones, L.; Burgin, T. P.; Zhou, C. W.; Muller, C. J.; Deshpande, M. R.; Reed, M. A.; Tour, J. M. *Nanotechnology* **1998**, *9*, 246−250.
(16) Nelson, J. C.; Saven, J. G.; Moore, J. S.; Wolynes, P. G. *Science* **1997**, *277*, 1793−1796.
(17) Prince, R. B.; Okada, T.; Moore, J. S. *Angew. Chem., Int. Ed. Engl.* **1999**, *38*, 233−236.
(18) Gin, M. S.; Yokozawa, T.; Prince, R. B.; Moore, J. S. *J. Am. Chem. Soc.* **1999**, *121*, 2643−2644.
(19) Prince, R. B.; Saven, J. G.; Wolynes, P. G.; Moore, J. S. *J. Am. Chem. Soc.* **1999**, *121*, 3114−3121.
(20) Grubbs, R. H.; Kratz, D. *Chem. Ber.* **1993**, *126*, 149−157.
(21) Shetty, A. S.; Zhang, J.; Moore, J. S. *J. Am. Chem. Soc.* **1996**, *118*, 1019−1027.
(22) Nelson, J. C. Ph.D. Thesis (Chemistry), University of Illinois, 1997.
(23) Mindyuk, O. Y.; Stetzer, M. R.; Heiney, P. A.; Nelson, J. C.; Moore, J. S. *Adv. Mater.* **1998**, *10*, 1363−1366.

10.1021/ja9909576 CCC: $18.00
Published on Web 06/10/1999

Chart 1

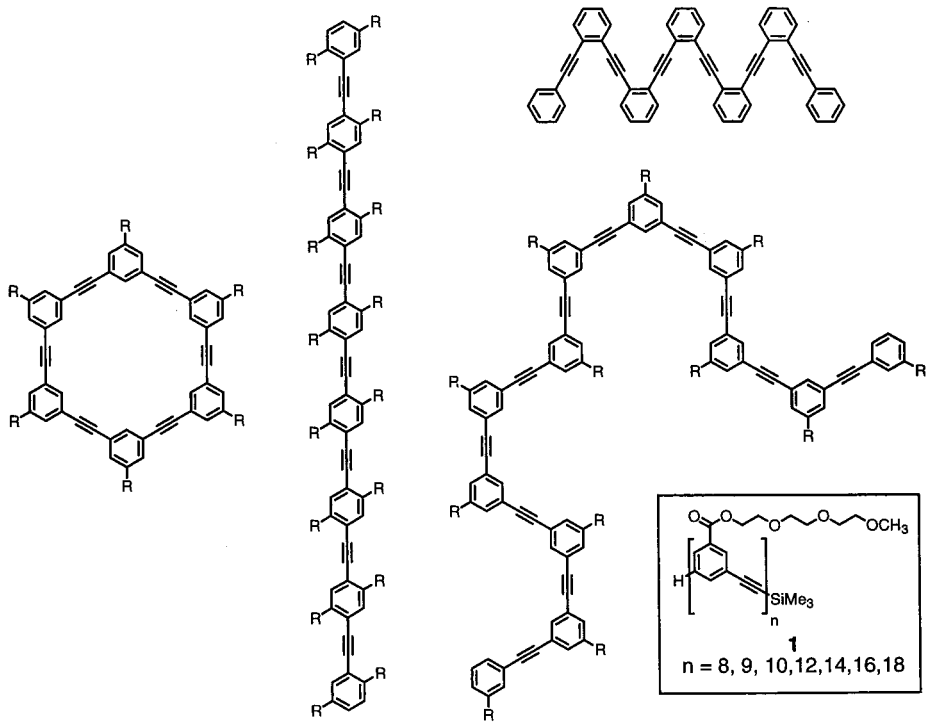

is in the form of stacked aggregates, analogous to the stacking of macrocycles (Figure 1).

In looking at this picture, we became curious about the supramolecular organization of the meta-oligomers in the absence of solvent. Two possible packing models were postulated at the outset of this study (Figure 1). On one hand, if the oligomers maintained the close analogy to their macrocyclic counterparts, one might expect that these helically disposed chains would self-organize into a tubular mesophase. On the other hand, a lamellar organization consisting of extended ribbon-like chains could achieve the favorable $\pi-\pi$ interactions without the costly free volume of the tubular phase. We describe below our investigations to elucidate the solid-state structure of *m*-phenylene ethynylene oligomers bearing ester-linked triethylene glycol side chains (**1**, Chart 1). These oligomers can be thought of as amphiphilic chain molecules having a flexible polar group appended to a rigid, aromatic hydrocarbon backbone. As described in detail below, this study was greatly facilitated by the availability of a series of oligomers of discrete size, which enabled systematic observations to be made as a function of chain length.

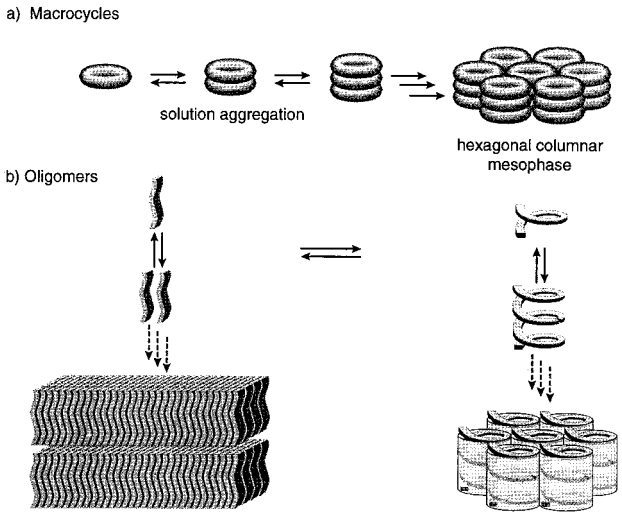

Figure 1. Schematic diagram illustrating the aggregation behavior of disk-shaped phenylene ethynylene macrocycles (a) and oligomers (b) over a wide range of concentration. In solution, the macrocycles undergo solvophobically driven intermolecular association.[21] In the absence of solvent, these extended-core mesogens self-organize into tubular discotic liquid crystal phases.[23] In dilute solution, ribbon-shaped oligomers of sufficient length fold back on themselves and adopt a helical conformation.[16−19] At higher concentrations, they associate intermolecularly,[22] possibly in the form of extended chain ribbons or as helical stacks.

Experimental Section

The synthesis, purification, and characterization of *m*-phenylene ethynylene oligomers, **1** (n = 8, 9, 10, 12, 14, 16, 18), were described elsewhere.[19] Melting point transitions were determined using a Linkam HFS91 hot stage and a Zeiss optical microscope at a heating rate of 5 °C·min^{-1}. All values were recorded as the midpoint of the thermal transition. Differential scanning calorimetry (DSC) was performed on a Perkin-Elmer Pyris1 under a nitrogen atmosphere. Transition enthalpies were calibrated against an indium standard. Temperature was calibrated with indium and with cyclohexane, which has two phase transitions (a total of three transitions were used for temperature calibration). The onset of melting transitions was obtained with a scan rate of 10 °C·min^{-1}, and the enthalpies were determined at a scan rate of 40 °C·min^{-1}.

Small- and wide-angle X-ray diffraction (SAXD and WAXD) measurements were performed with Cu Kα X-ray radiation (λ = 1.54 Å) calibrated to silver behenate. The X-ray generator was a Bruker M18XHF SRA rotating anode equipped with a 0.3-mm filament. All diffraction data were collected with Bruker Hi-Star area detectors. The sample-to-detector distance was 63.50 and 8.54 cm on the small-angle and wide-angle diffractometers, respectively. Samples were prepared in 0.7-mm glass capillaries by melting the oligomer on a vertical hotplate and utilizing capillary action and gravity to draw the melted sample inside. The samples were annealed by heating the capillaries under a nitrogen atmosphere to a temperature above the melting point, followed by slow cooling using an oil bath to regulate the temperature.

Aligned samples were prepared at room temperature by unidirectionally shearing the waxy solid on a flat Teflon block with a razor

Table 1. Thermal Transitions of **1**

n	mp (°C) optical microscopy[a]	mp (°C) DSC[b]	ΔH (kJ·mol^{-1} oligomer)
8	52	48	7.2
9	65		
10	77	73	21.2
12	94	87	28.6
14	106	94	29.8
16	113	104	31.6
18	119	110	43.7

[a] Measured by the loss of birefringence heating at a rate of 5 °C·min^{-1}. [b] Onset of endothermic transition heating at a rate of 10 °C·min^{-1}.

blade. The flattened sample was either rolled perpendicular to the shear direction (preparation method A) or cut into sheets perpendicular to the direction of the shear and stacked as sheets in a pile (preparation method B). These samples were placed into 1.0-mm capillaries and mounted in the path of the Cu Kα X-ray source. Samples prepared by method A had the X-ray beam perpendicular to the shear direction, while samples prepared by method B had the X-ray beam parallel to the shear direction.

The UV absorption spectra were recorded with a Shimadzu spectrophotometer (model UV-160A). Samples were prepared by spin-casting solutions of the decamer from CH_2Cl_2 at 4000 rpm for 20 s onto quartz slides. The thin films were annealed by heating the slides to 100 °C, holding the temperature constant for 1.5 h, and then slowly cooling to room temperature over 4 h.

Results

Oligomers **1** (n = 8, 9, 10, 12, 14, 16, 18) were viscoelastic waxes whose stiffness increased with increasing chain length. The tetramer and hexamer were oils that solidified below room temperature, and oligomers $n \geq 8$ were off-white, opaque solids at room temperature. Between crossed polarizers, these waxy solids showed strong birefringence, although no discernible liquid crystalline texture could be identified. Birefringence disappeared over a narrow temperature range upon heating and reappeared upon cooling. The reversibility of the phase transition was verified by the heating and cooling DSC traces (see Supporting Information). On heating, the DSC traces showed either a single transition or two coalesced transitions. On cooling, two exothermic transitions, separated by at most a few degrees, were typically observed. Based on either the transition onset for DSC heating curves or the temperature at which birefringence was lost, the melting point of the oligomers was found to increase monotonically as the chain length increased. The enthalpy of the transition (per mole of oligomer) also rose steadily as the oligomer lengthened. These data are summarized in Table 1 and plotted in Figure 2.

The solid-state structure was probed by small- and wide-angle X-ray measurements. Especially for the longer oligomers, the intensity and sharpness of the X-ray reflections were highly dependent on sample preparation. Oligomers that were simply melted into capillaries and cooled rapidly exhibited weak and broad (often indiscernible) reflections. In contrast, the diffraction peaks of samples cooled at slow rates were sharp and of much greater intensity. Table 2 lists the observed SAXD and WAXD d-spacings, and the corresponding integrated plots are shown in Figure 3. As the oligomer length increased, the value of the longest d-spacing increased. This small-angle reflection was assigned to the (100) plane. Second-order reflections were also observed, but they were significantly weaker. In contrast to the long spacings, the d-spacings for the other reflections remained nearly constant, regardless of chain length. The most prominent of these had d-spacings of about 20.0 and 3.6 Å.

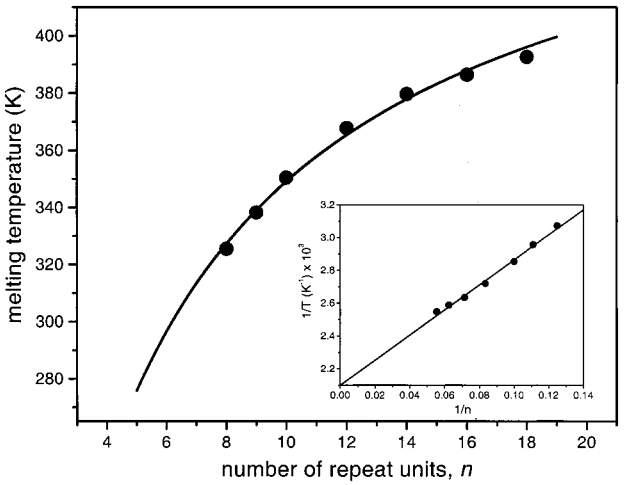

Figure 2. Melting transition from optical microscopy as a function of chain length, n. The inset shows a plot of $1/T$ vs $1/n$ and the corresponding linear fit (see eq 1). The asymptotic curve shown in the plot of T vs n was obtained from eq 1 using the parameters from linear regression (ΔH = 2.2 kJ·mol^{-1} repeat unit; T_m^{∞} = 476 K).

Table 2. Summary of X-ray Data

n	longitudinal spacings[a] (Å)				lateral spacings[b] (Å)		
8	47.1[c]	23.4[d]	10.9[e]		20.8[f]	4.4[g]	3.6
9	54.1[c]	26.7[d]	10.4[e]	5.7	20.1[f]	4.5[g]	3.6
10	59.6[c]	29.7[d]	10.2[e]	5.7	19.7[f]	4.5[g]	3.6
12	67.0[c]	32.9[d]	10.5[e]	5.8	19.9[f]	4.5[g]	3.6
14	76.4[c]	37.7[d]	10.4[e]	5.8	19.9[f]	4.5[g]	3.6
16	88.5[c]	42.7[d]	10.0[e]	5.8	19.9[f]	4.4[g]	3.6
18	97.6[c]	48.1[d]	10.1[e]	5.8	19.7[f]	4.5[g]	3.6

[a] Reflections that acquire orientation parallel to the shear direction. [b] Reflections that acquire orientation perpendicular to the shear direction. [c] (100) reflection. [d] (200) reflection. [e] Off-meridinal reflection. [f] Obtained from WAXD data. [g] Broad reflection.

At room temperature, these viscoelastic samples could be mechanically deformed and aligned by spreading or rolling the materials on flat substrates. Sheared samples exhibited macroscopic orientation as observed by X-ray diffraction patterns (Figure 4). The long spacing (100) and its second-order reflection (200) always aligned parallel to the direction of shear. With the sample mounted such that its shear direction was vertical (preparation A), the reflection corresponding to the long-spacing was diffracted along the meridian. The 20.0- and the 3.6-Å reflections for this orientation were diffracted along the equator. When the X-ray beam was oriented parallel to the shear direction (preparation B), the 3.6-Å reflection was diffracted along the meridian, while the 20.0-Å reflection was diffracted along the equator. These experiments show that the oligomers exhibit longitudinal as well as a bilateral order. As seen in Figure 4 and noted in Table 2, the reflection corresponding to a d-spacing of 10.4 Å lies off the meridian by roughly 30°.

Discussion

The phase transition of the oligomers was shown to increase with chain length in an asymptotic fashion. By analogy to conventional oligomers such as parafins,[24] this behavior implies that each of the discrete oligomers adopts a similar solid-state structure. Although only one odd-membered oligomer was examined (n = 9), it fell into place on the plot of T_m vs n, indicating a lack of odd−even effects (Figure 2). The melting point behavior of short-chain polymers can be treated classically

(24) Huggins, M. L. *J. Phys. Chem.* **1939**, *43*, 1083−1098.

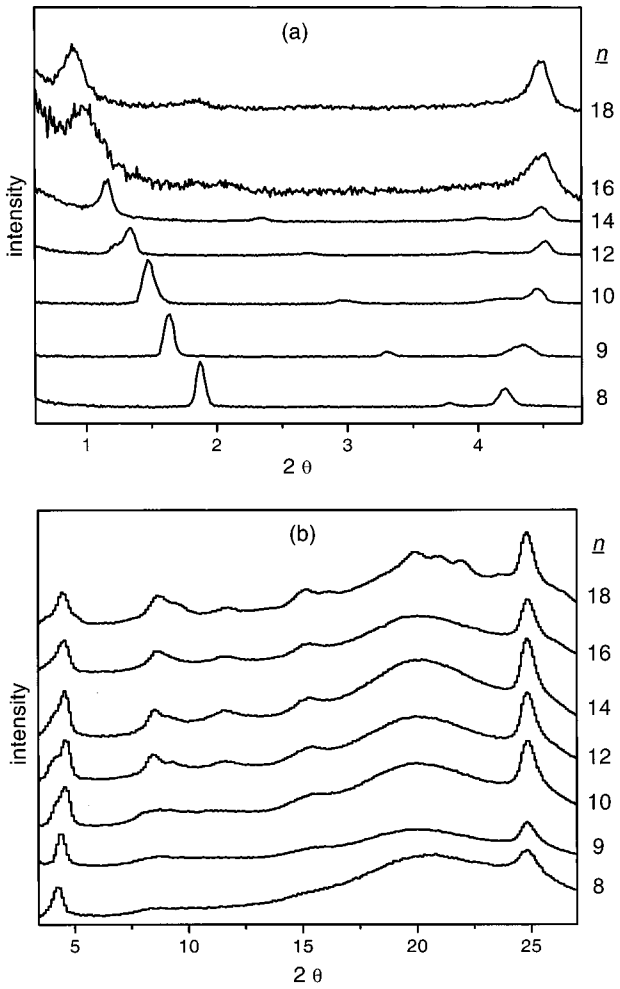

Figure 3. Small-angle (a) and wide-angle (b) X-ray diffraction profiles at room temperature of oligomers **1** ($n = 8-18$). All of the samples were prepared by slow cooling from the melt.

by considering chain ends to be impurities in the ordered phase.[25] Since the volume fraction of end groups is roughly inversely proportional to chain length, this approach leads to the relationship given in eq 1, where T_m is the melting temperature expressed in Kelvin, T_m^∞ is the melting point of a chain with infinite length, ΔH is the heat of fusion per mole of repeat unit, and n is the number of repeat units.

$$\frac{1}{T_m} = \frac{1}{T_m^\infty} + \frac{2R}{\Delta H}\frac{1}{n} \qquad (1)$$

The inset in Figure 2 shows that a linear correlation is obtained when the inverse of the melting temperature is plotted against the inverse of the chain length. From the intercept, T_m^∞ is estimated to be 203 °C, and from the slope, ΔH is estimated to be 2.2 kJ·mol^{-1} of repeat unit. This value can be compared to enthalpy values obtained by DSC. Using the data in Table 1, a plot of ΔH (per mole of oligomer) vs n gives an approximately linear correlation with a slope of 3.1 kJ·mol^{-1} repeat unit, in reasonable agreement with the value from the melting point data.

At the start of this work, two possible models of solid-state organization were envisioned (Figure 1). We also imagined that packing might switch from a lamellar to a helical organization once the chain became long enough to stabilize the helical conformation. Although transition temperatures in both the lamellar and the helical organizations should be subject to melting point depression from end group irregularities, the observed smooth rise in melting transition with increasing chain length implies that only one type of packing is adopted for the entire series. In other words, there does not appear to be an abrupt switch in organization as the chain grows from $n = 8$ 18. It should be noted that, in dilute solution, we observe a stable helix for $n > 8$ in polar solvents. To establish which, if either, of the postulated organizations shown in Figure 1 was adopted, we turned our attention to X-ray diffraction studies.

The long spacings obtained from SAXD data were plotted against the number of repeat units, n, as shown in Figure 5. A linear relationship was observed with a slope of 4.93 Å and a y-intercept of 8.8 Å. The slope corresponds to the amount that each repeat unit extends the long spacing, while the y-intercept describes the end group contribution. The fact that each repeat adds such a large increment (i.e., 4.93 Å) to the long spacing rules out the helical packing model shown in Figure 1; the observed behavior is consistent with a lamellar packing model. The calculated length of the repeat unit based on molecular models is 5.75 Å, a value significantly larger than that obtained from the slope of the plot in Figure 5. This discrepancy can be reconciled by assuming that the backbone packs at an offset angle of roughly 30° with respect to the layer normal. Although there are an infinite number of directions about which to tilt the chain, the one that is most obvious for this particular molecular geometry involves rotating the chain 30° about the normal to the aromatic stacking direction (i.e., the 3.6 Å reflection). This orientation aligns the oligomer in a "stair step" fashion with respect to the lamellar normal (Figure 6). A molecular model of this packing arrangement was constructed and found to be physically reasonable (see Supporting Information). This model provides about the right amount of space for interdigitation of the triethylene glycol side chains.

While the longitudinal spacing increased with oligomer chain length, the lateral reflections remained constant. Based on the molecular model mentioned above, we correlated the 20.0 Å spacing to Bragg planes separating equivalent segments of adjacent oligomers. This distance corresponds to the space required by the interdigitating side chains. From macroscopically oriented diffraction data, the 3.6 Å spacing was shown to be orthogonal to the 20.0 Å reflection and corresponds to a distance consistent with aromatic face-to-face stacking. Assuming a monoclinic cell with $\beta = 120$ ° and edges of $(2/3^{1/2})(4.93n + 8.8)$, 20.0, and 3.6 Å for each oligomer, the average density (assuming one molecule per cell) was estimated to be 1.2 g·cm^{-3}. Although we did not explicitly measure the density, this value is reasonable, given the elemental composition of these oligomers.

These viscoelastic waxy materials could easily be aligned at room temperature by shearing the samples. This process not only induces alignment in the longitudinal direction, but it also produces bilateral alignment. As expected, the long axis aligns in the direction of shear. Moreover, the 20.0 Å lateral spacing has a slight preference to adopt an orientation perpendicular to the shear plane, while the 3.6 Å spacing has a preference to remain in the shear plane. It is also interesting to note that the 10.4 Å reflection lies off the meridian. This reflection is likely associated with Bragg planes along the chain direction.

We have previously used UV absorption spectroscopy to study the conformation of these oligomers in solution.[16-19] Given that the conformation in the solid state has been reasonably well established by the X-ray analysis described above, we wanted to compare the UV spectra of the oligomers

(25) Flory, P. J. *Principles of Polymer Chemistry*; Cornell University Press: Ithaca, NY, 1953.

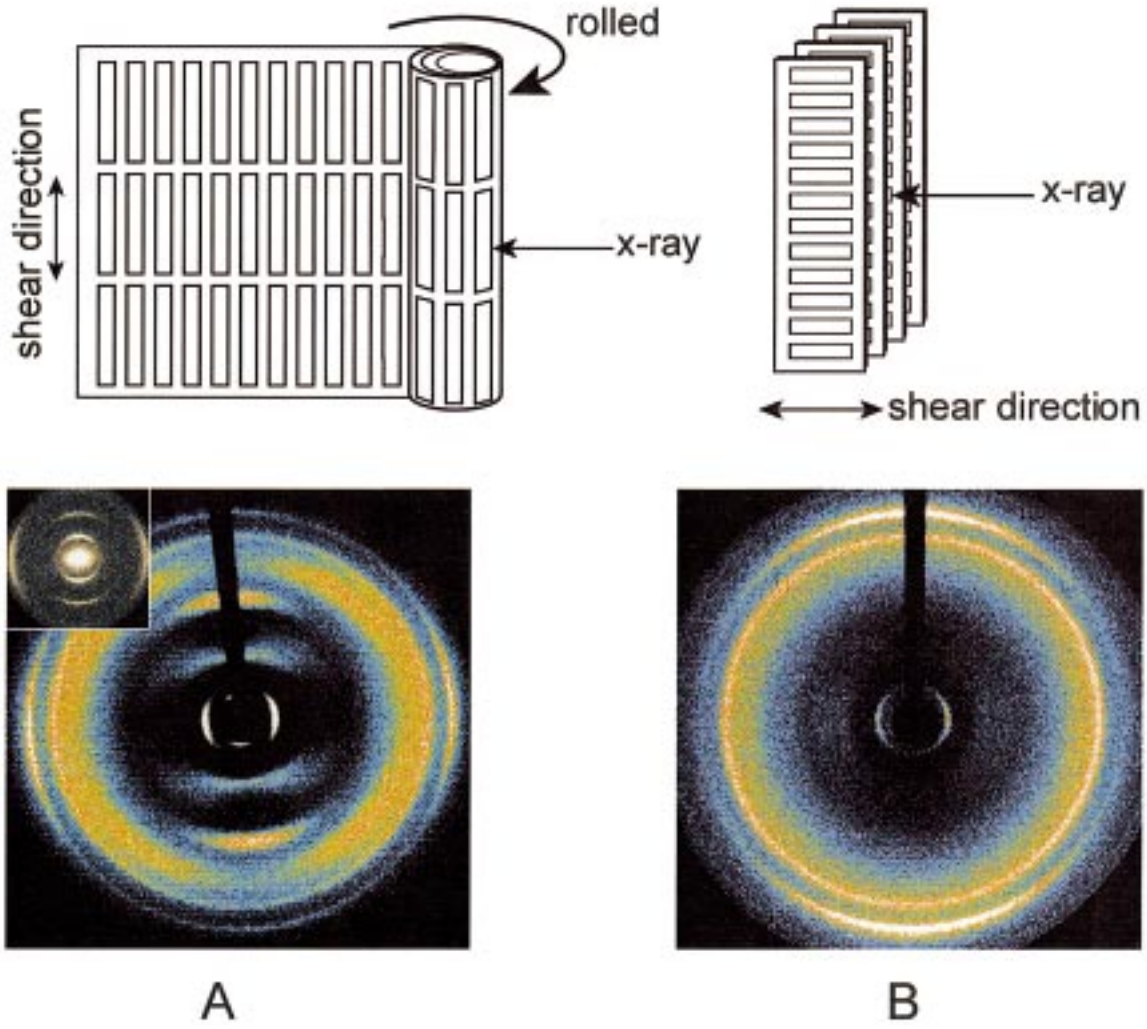

Figure 4. Wide-angle X-ray patterns of shear-aligned samples of **1** ($n = 10$). The X-ray patterns labeled "A" were recorded on a sample obtained by rolling up a sheared film along a direction perpendicular to the shear. The resulting cylinder was oriented in the X-ray beam with its long axis (i.e., the shear direction) vertical (see A). The inset shows the small-angle diagram. The X-ray pattern labeled "B" was obtained by cutting a sheared film into strips along a direction perpendicular to the shear direction. The strips were stacked atop one another, and the sample was placed in the X-ray beam such that the stacking direction was horizontal and the X-ray beam was parallel to the direction of the shear (see B).

in the thin films to their spectra in dilute solution (Figure 7). In $CHCl_3$, the spectrum of the $n = 10$ oligomer shows two bands with maxima at 290 and 303 nm. In this solvent, the backbone is believed to be in a random conformation that consists of a mixture of cisoid and transoid states (eq 2). In CH_3CN, where

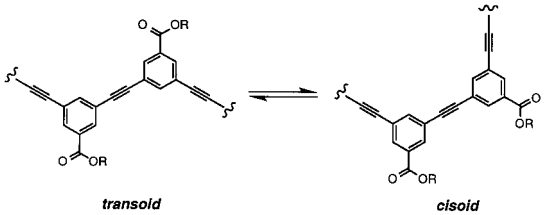

(2)

the conformation is believed to be helical (predominantly cisoid), the UV spectrum shows decreased absorbance in the 303 nm band relative to the 290 nm band. UV spectra of thin films were broad and red shifted. The solid-state spectra were also found to be dependent on thermal annealing. Samples of $n = 10$ spin cast from solution and annealed just below the melting point gave the spectrum shown in Figure 7. While broadening makes

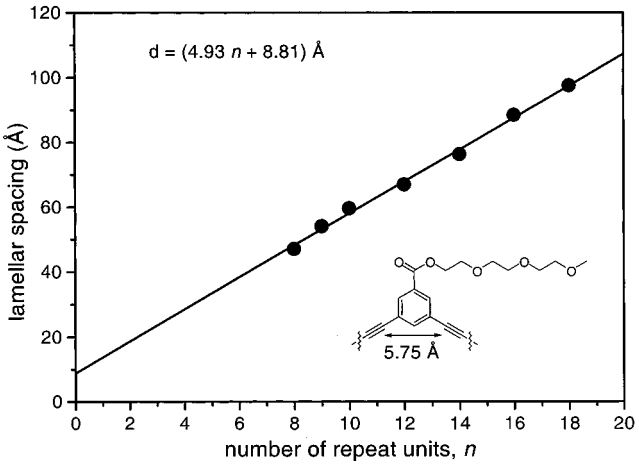

Figure 5. Lamellar spacing obtained from SAXD measurements plotted against chain length. The solid line is a linear fit to the data (i.e., $d = (4.93n + 8.8)$ Å). The slope corresponds to the incremental thickness per repeat unit, and the intercept gives the end group contribution. Molecular models indicate a repeat unit distance of 5.75 Å as shown.

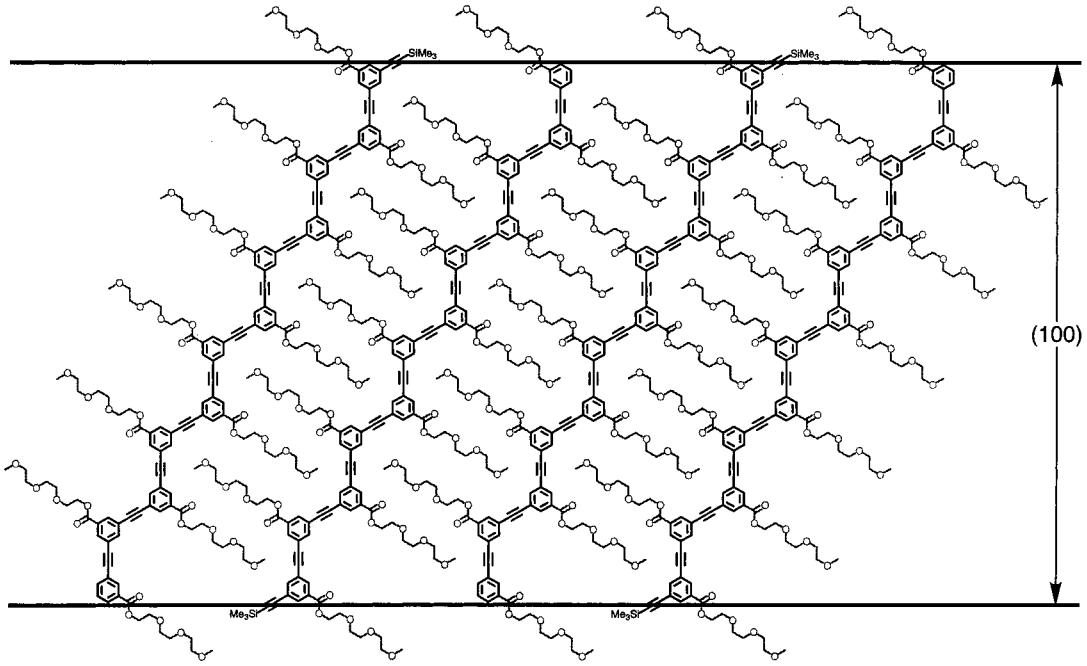

Figure 6. Schematic diagram of the packing model.

interpretation difficult, it is possible to identify two maxima at 294 and 307 nm. The ratio of these peak intensities in the annealed films is more similar to those in $CHCl_3$, in which there is a high population of transoid conformers. This is the expected conformation based on the X-ray interpretation described above.

Considering the two limiting models shown in Figure 1, it may not be surprising that the lamellar arrangement is the thermodynamically favored organization. This organization clearly has a much higher density and is free of the channel void space. It is interesting that the samples used for both the X-ray and UV studies were strongly influenced by thermal annealing, a process that was necessary to bring about order in the solid state. This was particularly important for the largest oligomers, as they showed no X-ray reflections unless they were slowly cooled from the melt. Based on these observations, it appears that significant conformational changes take place in order to acquire the thermodynamically stable lamellar organization.

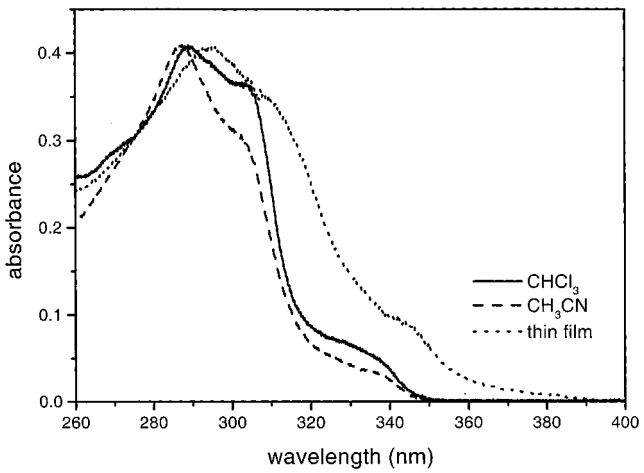

Figure 7. UV absorption spectra of **1** ($n = 10$) in solution and thin films. Thin-film spectra were recorded after annealing the samples by slow cooling from just below the melting point. The spectra were normalized to a constant absorbance at their λ_{max}.

The results presented here suggest interesting possibilities for controlling solid-state and solution organizations. For example, in solution, oligomers tethered by a short, flexible segment might acquire either a helical dimer structure or a parallel ribbon arrangement. In the solid-state, the strong preference of these oligomers to adopt smectic-like lamellar organizations and the ease at which they shear align might be used to design phases that acquire spontaneous polar order. We are currently pursuing some of these ideas and will report on them in the future.

Conclusions

Systematic studies on amphiphilic phenylene ethynylene oligomers of discrete size have yielded a detailed picture of their solid-state packing. These waxy solids exhibited thermal phase transitions that rose asymptotically in temperature as the chain lengthened. Such behavior implied a homologous mode of packing for all members of the series, reminiscent of conventional short-chain homopolymers whose transition temperatures are dominated by melting point depression from end group irregularities. Small- and wide-angle X-ray diffraction studies performed on slow-cooled samples provided evidence for lamellar organization. In particular, the long *d*-spacing and its second-order reflection grew in direct proportion to chain length and hence was assigned to the lamellar thickness. The discrepancy between the fully extended chain length and the lamellar thickness was reconciled by assuming an approximate 30° tilt of the chain with respect to the layer normal. Unlike smectic liquid crystals, these viscoelastic substances acquired bilateral order, as evidenced from shear aligned samples. The schematic diagram of lamellar organization shown in Figure 1 thus represents a nearly accurate depiction of the structure adopted by these oligomers, except that it fails to reveal the tilting of the backbone. The strong tendency of these chains to adopt lamellar order, together with their ability to be aligned macroscopically, may provide a useful strategy to realize polar phases and other supramolecular structures.

Acknowledgment. We thank Eun-Sil Jung for conducting preliminary measurements, and we acknowledge the Laboratory of Macromolecular and Organic Chemistry at Eindhoven

University of Technology for the use of its DSC. This material is based upon work supported in part by the National Science Foundation (NSF DMR 98-08433) and by the U.S. Department of Energy, Division of Materials Sciences, under award no. DEFG02-96ER45439 through the Frederick Seitz Materials Research Laboratory at The University of Illinois at Urbana−Champaign. R.B.P. thanks the Lubrizol Corp. for a fellowship.

Supporting Information Available: Representative DSC traces and a figure showing the chain packing model (PDF). This material is available free of charge via the Internet at http://pubs.acs.org.

JA9909576